Nanostructures

DOI: 10.1002/anie.200901447

Etching and Growth: An Intertwined Pathway to Silver Nanocrystals with Exotic Shapes**

*Claire M. Cobley, Matthew Rycenga, Fei Zhou, Zhi-Yuan Li, and Younan Xia**

Shape-controlled synthesis has proven to be a powerful means for controlling the properties of metal nanocrystals and optimizing them for applications in catalysis,[1] electronics,[2] sensing,[3] biomedical imaging,[4] and surface-enhanced Raman scattering (SERS).[5] By careful control of reaction conditions (e.g., reaction temperature, surface capping, and concentrations of reagents and ionic species), nanocrystals with a wide variety of shapes have been synthesized.[6] However, the majority of nanocrystals that have been prepared to date are highly symmetric, limited to the face-centered cubic lattice assumed by most metals. Of the anisotropic shapes that have been observed, the majority (e.g., bars, rods, and wires) are due to preferential growth along a single direction.[2,7,8] To increase the diversity of nanocrystal shapes, we need to find new routes to break the cubic symmetry and thus force the growth process into other anisotropic modes.

Recently, seeded overgrowth has been demonstrated as a versatile route to the formation of nanocrystals with both simple and complex shapes and compositions, including bimetallic nanoparticles.[9,10] A typical example is the transformation of silver nanocubes into their geometric dual octahedrons, as a result of preferential overgrowth at all {100} facets.[10] Herein, we present an etching-induced growth mechanism by which silver nanocubes are transformed into nanocrystals with an exotic shape, namely anisotropically truncated octahedrons. In this case, the overgrowth occurs preferentially on three adjacent faces that share a corner, which is slightly truncated owing to oxidative etching (Figure 1). This preferential overgrowth results in a non-centrosymmetric shape, although the single-crystal structure is preserved.

The synthesis started with a typical sulfide-mediated polyol process for silver nanocubes.[11] At the end of this process, a second aliquot of silver nitrate ($AgNO_3$) solution was added and to our surprise, the cubic nanocrystals were found to evolve into anisotropically truncated octahedrons, a shape of lower symmetry relative to a cube or octahedron. Figure 1 shows electron micrographs of silver nanoparticles before and after the second aliquot of $AgNO_3$ solution was introduced. The sulfide-mediated synthesis resulted in a uniform sample of silver nanocubes 46 nm in edge length (Figure 1a). Ten minutes after the addition of the second aliquot of $AgNO_3$ solution, essentially all the silver cubes had been transformed into anisotropically truncated octahedrons of 68 nm in size as measured along the longest edge (Figure 1b). Unlike a regular octahedron, three adjacent corners of this new nanocrystal are snipped significantly (Figure 1c).

It has previously been shown that gradual addition, over two hours, of $AgNO_3$ and PVP solutions to the product of a conventional polyol synthesis could facilitate the transformation of silver cubes of 80 nm in edge length into octahedrons of 300 nm in size.[10] This shape transformation could be attributed to faster addition of silver atoms to the {100} faces

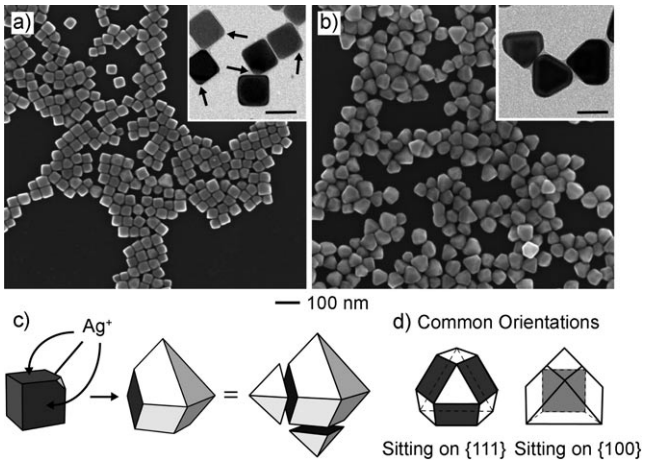

Figure 1. When a second aliquot of $AgNO_3$ was introduced at the end of a sulfide-mediated polyol synthesis, the Ag nanocubes evolved rapidly into a new anisotropic structure. a),b) SEM images with TEM insets of the product before (a) and 10 min after introduction of additional $AgNO_3$ (b); scale bars in the insets: 50 nm. The arrows indicate the corners of nanocubes that have been truncated owing to oxidative etching. c) A proposed mechanism for this transformation. Silver ions reduced more rapidly on three {100} faces adjacent to the truncated corner, leading to the formation of an anisotropically truncated octahedron. For comparison, an octahedron is also shown with three of the corners removed. Note that the third detached corner is not visible at this orientation. White and gray denote {111} and {100} facets, respectively. d) The two most common orientations of the anisotropically truncated octahedron on a flat substrate, as viewed from above.

[*] C. M. Cobley, M. Rycenga, Prof. Y. Xia
Department of Biomedical Engineering, Washington University
St. Louis, MO 63130 (USA)
E-mail: xia@biomed.wustl.edu
F. Zhou, Prof. Z.-Y. Li
Institute of Physics, Chinese Academy of Sciences
Beijing 100080 (China)

[**] This work was supported in part by the NSF (DMR-0804088), an NIH Director's Pioneer Award (DP1 OD000798), and startup funds from Washington University in St. Louis. Z.Y.L. would like to acknowledge financial support from the National Natural Science Foundation of China (10525419, 60736041, and 10874238).
Supporting information for this article is available on the WWW under http://dx.doi.org/10.1002/anie.200901447.

of the cube than the {111} capped corners. In the present work, we propose that the same principle of more rapid growth on {100} faces is still valid, but in a much less symmetrical pattern. Instead of being added to all six faces of the cube evenly, the silver atoms were added to three adjacent {100} faces more rapidly than the other three {100} faces. Figure 1c shows a schematic of this new growth mechanism, where white and gray signify the {111} and {100} facets, respectively. The three fast-growing {100} faces are determined by a slightly truncated corner, which is believed to be the reason for the highly anisotropic growth. As a result, half of the cube grows into an octahedron, while the other half retains a truncated cubic morphology. When sitting on a substrate, such an exotic nanocrystal typically takes on one of two orientations. Either it sits on the large {111} facet on the 'octahedron side' of the crystal, or it sits on one of the three square {100} facets. Figure 1d shows these orientations which match the images obtained from SEM and TEM (Figure 1b).

The formation of silver nanocubes that serve as the seeds and the subsequent growth into anisotropically truncated octahedrons are rapid processes. The presence of sulfide species, in this case HS^-, results in accelerated growth of the cubes in the first step owing to the generation of silver sulfide, a catalyst for silver reduction.[12] The reaction involved in the second step is also rapid; the injection of $AgNO_3$ takes less than a minute and the final product is obtained 10 minutes later. This rapid rate makes it possible for the final shape to be kinetically determined instead of being the thermodynamically favored shape (cubo-octahedron or a truncated octahedron) at this size. To confirm the importance of this rapid growth, a similar experiment was performed, where the second aliquot of $AgNO_3$ was added 15 times slower (at a rate of $0.05\,mL\,min^{-1}$ rather than $0.75\,mL\,min^{-1}$). Instead of growing anisotropically, the silver atoms were added uniformly to all six {100} faces, retaining the cubic morphology during overgrowth (Supporting Information, Figure S1a).

Oxidative etching is also an important factor in determining the final shape of nanocrystals obtained in a solution-phase synthesis and has been proposed as a basis for the activation of specific face(s) of a nanocrystal for further growth.[6,13] In our previous work, both a rapid reduction rate and localized oxidative etching were shown to be critical to break the cubic symmetry and promote anisotropic growth of silver and palladium cubes into rods or bars. Adding a capping agent that prevents oxidative etching was shown to shorten the palladium nanobars significantly, resulting in a cubic shape.[13] Etching may also play a role in the synthesis of silver nanobars as increased concentrations of the etchant (Br^-) were necessary for their growth.[7] A similar mechanism appears to be responsible for the anisotropic growth observed in the present study, although with a significant difference. Instead of a single face being activated for further growth, the etching of one corner of the cube promotes growth of all three adjacent faces that share this corner. Mild etching is known to occur in the late stages of a sulfide-mediated silver nanocube synthesis. The corners of the cubes have been shown to be irregular (that is, they are not all evenly etched) if the reaction was left unquenched after all the $AgNO_3$ had been consumed.[11] As indicated by arrows in the inset of Figure 1a, a number of particles with uneven corner truncation could be seen in the TEM images of the seed cubes. A closer examination of multiple micrographs of the nanocubes in Figure 1a indicates that approximately 20% of them appear to be truncated at one corner. Observation of this truncation is, however, not expected on every cube as the contrast difference can be small if the truncations are not significant. The silver atoms that are dissolved from the region of the etched corner of a cube are likely to be redeposited in a nearby area, activating the adjacent three faces for further growth once additional $AgNO_3$ is introduced. The stirring in this reaction is mild and thus should allow for local forces to play a significant role. To confirm the importance of oxidative etching in our mechanism, the same reaction was performed in an argon-saturated solution. In this case, no shape transformation was observed and the final product was simply silver nanocubes (Supporting Information, Figure S1b) as no face was preferentially activated.

To confirm our assignment of this unusual shape, extensive electron microscopy analysis was performed and all the results were consistent with an anisotropically truncated octahedron. Other geometries were also investigated, includ-

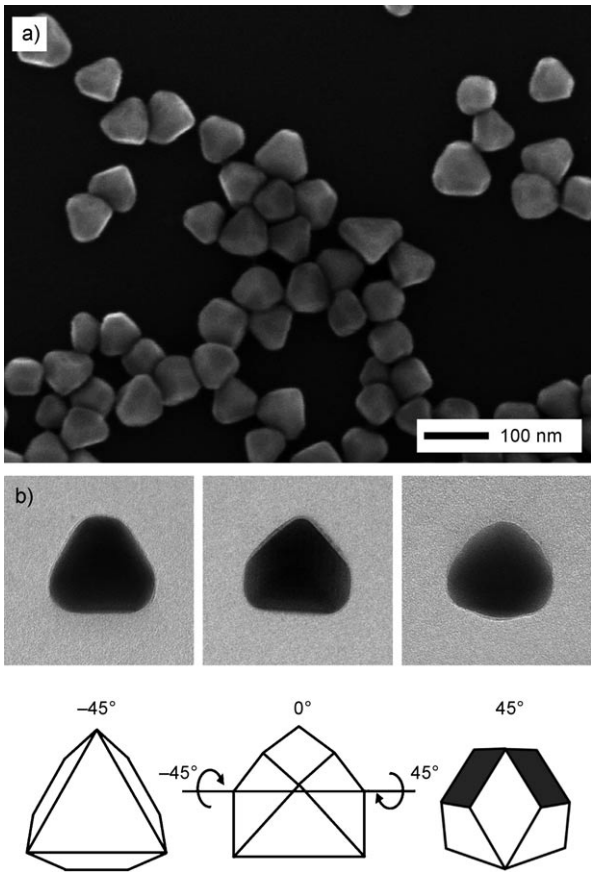

Figure 2. a) A high-magnification SEM image of the anisotropically truncated octahedrons of Ag with well-developed facets. b) TEM images taken from a single anisotropically truncated octahedron at three different tilting angles and diagrams of a model that has been tilted by the same amount (the directions of rotations are indicated by the arrows). White and gray signify {111} and {100} facets, respectively.

ing bipyramids, truncated tetrahedrons, and unevenly truncated cubes, but none of them could explain all the data presented herein. Figure 2a shows a high-magnification SEM image, in which the faceted nanocrystals are better resolved. This image clearly shows multiple examples of the two most common profiles of the nanocrystals: 'houses' and triangles. A typical 'house' orientation is shown in Figure 2b at three different tilting angles, and a model is presented for comparison. The two sets of images match closely, though the edges and the corners of the actual nanocrystals appear slightly rounded in comparison with the idealized model owing to corner truncation. Further tilting of this model also suggests that the seemingly non-uniform appearance of the sample is most likely caused by its highly anisotropic nature (Supporting Information, Figure S2).

High-resolution TEM analysis in Figure 3 validates the single-crystal structure of the product, confirms the presence of both {100} and {111} facets, and verifies the fringe spacings expected from the model at different orientations. Figure 3a, b, shows the analysis of a nanocrystal sitting on the large triangular face bound by a {111} plane. The fringe spacing of 1.4 Å can be indexed to the {220} reflection of silver. The inset in Figure 3b shows a fast Fourier transform (FFT) of the high-resolution image, where the spots have a six-fold symmetry and can be indexed to the {220} reflection, indicating that the nanocrystal was sitting on a {111} face. Figure 3c, d, shows the analysis of a nanocrystal sitting on a square {100} face. The fringe spacing of 2.0 Å corresponds to the {200} reflection of silver. The FFT pattern in the inset shows a square symmetry and spots for both the {200} and {220} reflections, indicating that the nanocrystal is sitting on a {100} face.

Figure 4a shows UV/Vis spectra recorded from solutions of the two different stages depicted in Figure 1. After the second $AgNO_3$ aliquot was added, the primary peak red-shifted by 25 nm, as would be expected for a size increase, and a new peak developed at 380 nm between the two peaks seen in the spectrum for nanocubes. Previously, discrete-dipole approximation (DDA) calculations for 40 nm silver cubes and octahedrons showed that the main peak for octahedrons is located between the two peaks of a similarly sized cube as we see in this case, supporting our claim that our structure is a hybrid between a cube and an octahedron.[14] DDA calculations for an anisotropically truncated octahedron were performed (Supporting Information, Figure S3). We used 3424 dipoles and the three sharp points of the 'octahedron side' were snipped by 11.7 nm to reflect the slightly truncated nature of the particle and to match the experimental spectra. As shown in Figure 4b, the same overall shape can be seen with a clear shoulder at 380 nm.

The unusual nanocrystals were further investigated for SERS applications. Silver is an ideal substrate for SERS owing to its high polarizability, and can provide enhancement factors an order of magnitude larger than other metals, such as gold.[15] Furthermore, nanocrystals with sharp tips, such as the points of an octahedron, can concentrate the field into small volumes and thus create regions with higher enhancement.[16] However, it is still not clear if the sharp corners need to be positioned in a specific configuration to generate a strong, localized electric field. We performed some preliminary measurements with 1,4-benzenedithiol (1,4-BDT) and a 514 nm laser to test the SERS capabilities of the new nanocrystals. Well-resolved spectra could be easily obtained and a typical example of the solution-phase spectrum is shown in Figure 4c, from which an enhancement factor of 7.5×10^3 was obtained for the 9a ring breathing vibration at 1183 cm^{-1}. Single-particle SERS spectra could also be obtained and a typical example is shown in Figure 4d. Interestingly, despite the sharp corners, the overall enhancement factor was slightly lower than that predicted based on the studies of silver nanocubes of similar sizes.[16] This result probably arises because although the nanocrystal has sharp corners, all of them are opposite a flat face instead of another corner, leading to a weaker dipole polarization. In this regard, the availability of silver nanocrystals with sharp corners and different

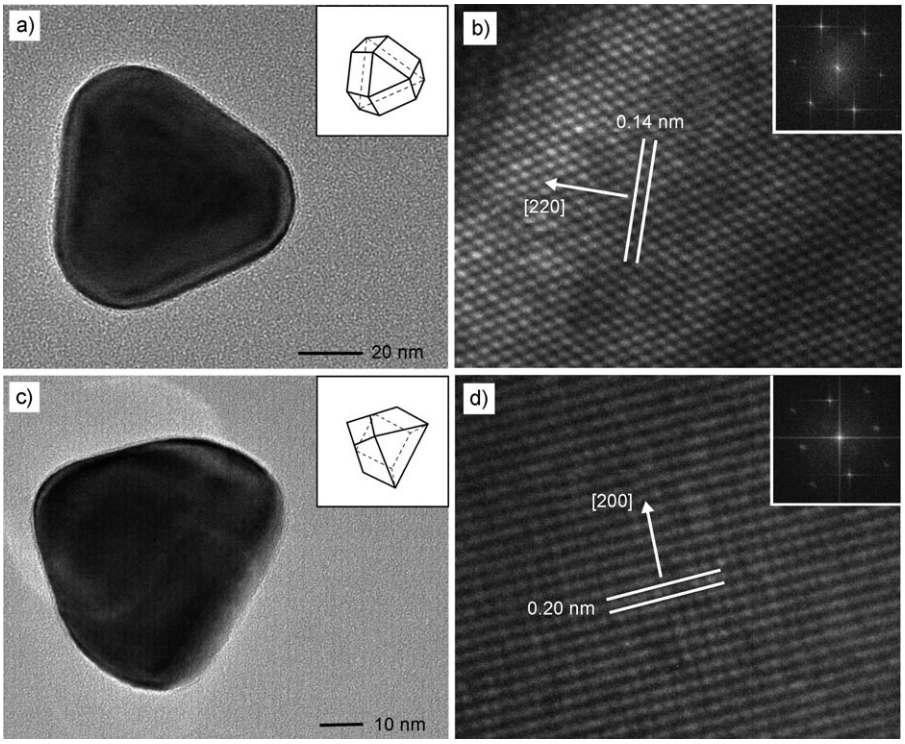

Figure 3. High-resolution TEM analysis of the two orientations typically observed, with the anisotropically truncated octahedron sitting on a), b) a triangular {111} face and c), d) a square {100} face. Insets for (a) and (c): models of the anisotropically truncated octahedron at that orientation. Insets for (b) and (d): fast Fourier transform (FFT) patterns of the high-resolution TEM images.

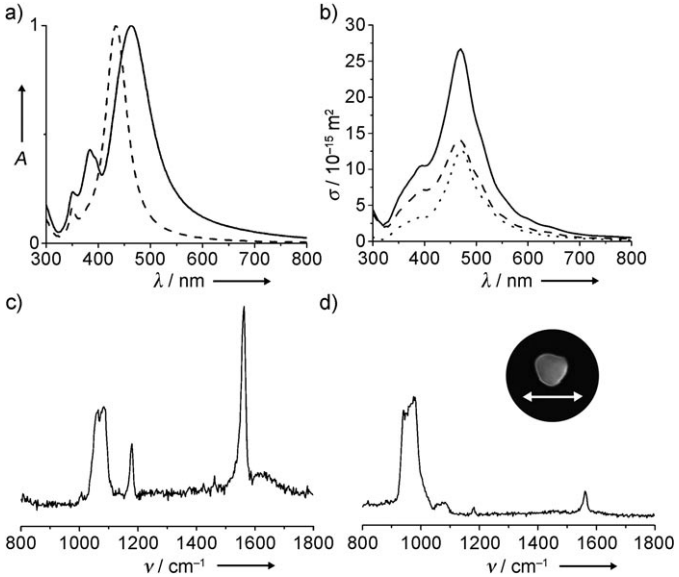

Figure 4. a) Normalized UV/Vis spectra of aqueous suspensions of the Ag nanocubes (-----) and the corresponding product of anisotropically-truncated octahedrons (——). b) DDA calculations of the extinction (——), absorption (-----), and scattering (•••••) cross section (σ) for an anisotropically truncated octahedron suspended in water with random orientations. The sharp corners were snipped by 11.7 nm to reflect the slightly truncated nature to provide better fit with the experimental data. c) Solution phase SERS spectrum of 1,4-BDT adsorbed onto the surface of the anisotropically-truncated octahedrons. The overlapping peaks at 1067 cm^{-1} and 1085 cm^{-1} are attributed to the fundamental benzene ring breathing mode 1, the peak at 1182 cm^{-1} is attributed to the 9a ring breathing vibration, and the peak at 1563 cm^{-1} is attributed to the 8a ring breathing vibration. d) Single-particle SERS spectrum of 1,4-BDT adsorbed on the anisotropically truncated octahedron shown in the inset. In addition to the peaks seen in (c), a broad peak just below 1000 cm^{-1} is visible, which can be ascribed to the silicon substrate. The polarization direction is indicated by the white arrow.

symmetries would provide a set of ideal substrates for better understanding the SERS phenomenon.

In summary, we demonstrated anisotropic overgrowth that proceeds more quickly from three adjacent faces that share a single corner of a nanocube. The overgrowth was activated owing to oxidative etching of this shared corner. Rapid reduction was also found to be a key factor in this unique shape transformation. The final products were anisotropically truncated octahedrons, which showed a noncentrosymmetric shape with interesting features for fundamental studies of SERS.

Experimental Section

Ethylene glycol (EG, 6 mL) was preheated for 1 h in a 24 mL vial at 152 °C. At this point, sodium hydrosulfide solution (3 mM, 70 μL) in EG was injected, and 8 min later a poly(vinyl pyrrolidone) solution (30 mg in 1.5 mL EG) and a $AgNO_3$ solution (24 mg in 0.5 mL EG). After 10 min, an aliquot was taken with a glass pipette through a small hole that had been drilled in the cap. Next, an additional aliquot of $AgNO_3$ solution (24 mg in 0.5 mL EG) was added using a syringe pump at a rate of 0.75 mL min^{-1} (0.05 mL min^{-1} for the control experiment), also through the hole in the cap. After 10 min, the reaction was quenched in an ice bath and the product was washed with acetone and water. For argon-protected syntheses, the preheated EG and all solutions were purged with argon for 1 h and argon flow was maintained over the surface during the reaction. Additional details are available in the Supporting Information.

Received: March 16, 2009
Published online: May 28, 2009

Keywords: nanocrystals · oxidative etching · surface-enhanced Raman scattering · silver

[1] a) J. D. Aiken III, R. G. Finke, *J. Mol. Catal. A* **1999**, *145*, 1; b) L. N. Lewis, *Chem. Rev.* **1993**, *93*, 2693.
[2] Y. Xia, P. Yang, Y. Sun, Y. Wu, B. Mayers, B. Gates, *Adv. Mater.* **2003**, *15*, 353.
[3] a) N. L. Rosi, C. A. Mirkin, *Chem. Rev.* **2005**, *105*, 1547; b) M. C. Daniel, D. Astruc, *Chem. Rev.* **2004**, *104*, 293.
[4] a) M. Hu, J. Chen, Z. Y. Li, L. Au, G. V. Hartland, X. Li, M. Marquez, Y. Xia, *Chem. Soc. Rev.* **2006**, *35*, 1084; b) J. L. West, N. J. Halas, *Annu. Rev. Biomed. Eng.* **2003**, *5*, 285.
[5] a) S. Nie, S. Emory, *Science* **1997**, *275*, 1102; b) C. L. Haynes, R. P. Van Duyne, *J. Phys. Chem. B* **2001**, *105*, 5599.
[6] Y. Xia, Y. Xiong, B. Lim, S. E. Skrabalak, *Angew. Chem.* **2009**, *121*, 62; *Angew. Chem. Int. Ed.* **2009**, *48*, 60.
[7] B. J. Wiley, Y. Chen, J. M. McLellan, Y. Xiong, Z.-Y. Li, D. Ginger, Y. Xia, *Nano Lett.* **2007**, *7*, 1032.
[8] C. J. Murphy, T. K. Sau, A. M. Gole, C. J. Orendorff, J. Gao, L. Gou, S. E. Hunyadi, T. Li, *J. Phys. Chem. B* **2005**, *109*, 13857.
[9] a) B. Lim, X. Lu, M. Jiang, P. H. C. Camargo, E. C. Cho, E. P. Lee, Y. Xia, *Nano Lett.* **2008**, *8*, 4043; b) S. E. Habas, H. Lee, V. Radmilovic, G. A. Somorjai, P. Yang, *Nat. Mater.* **2007**, *6*, 692; c) F. R. Fan, D. Y. Liu, Y. F. Wu, S. Duan, Z. X. Xie, Z. Y. Jiang, Z. Q. Tian, *J. Am. Chem. Soc.* **2008**, *130*, 6949; d) J. Burt, J. Elechiguerra, J. Reyesgasga, J. Martinmontejanocarrizales, M. Joseyacaman, *J. Cryst. Growth* **2005**, *285*, 681; e) D. Seo, C. I. Yoo, J. Jung, H. Song, *J. Am. Chem. Soc.* **2008**, *130*, 2940; f) S. E. Skrabalak, Y. Xia, *ACS Nano* **2009**, *3*, 10.
[10] a) A. Tao, P. Sinsermsuksakul, P. Yang, *Angew. Chem.* **2006**, *118*, 4713; *Angew. Chem. Int. Ed.* **2006**, *45*, 4597; b) A. R. Tao, D. P. Ceperley, P. Sinsermsuksakul, A. R. Neureuther, P. Yang, *Nano Lett.* **2008**, *8*, 4033; c) D. Seo, C. I. Yoo, J. C. Park, S. M. Park, S. Ryu, H. Song, *Angew. Chem.* **2008**, *120*, 775; *Angew. Chem. Int. Ed.* **2008**, *47*, 763.
[11] A. Siekkinen, J. M. McLellan, J. Chen, Y. Xia, *Chem. Phys. Lett.* **2006**, *432*, 491.
[12] A. Kryukov, A. Stroyuk, N. Zinchuk, A. Korzhak, S. Kuchmii, *J. Mol. Catal. A* **2004**, *221*, 209.
[13] Y. Xiong, H. Cai, B. J. Wiley, J. Wang, M. J. Kim, Y. Xia, *J. Am. Chem. Soc.* **2007**, *129*, 3665.
[14] B. J. Wiley, S. H. Im, Z.-Y. Li, J. M. McLellan, A. R. Siekkinen, Y. Xia, *J. Phys. Chem. B* **2006**, *110*, 15666.
[15] M. Quinten, *Appl. Phys. B* **2001**, *73*, 245.
[16] J. M. McLellan, Z.-Y. Li, A. R. Siekkinen, Y. Xia, *Nano Lett.* **2007**, *7*, 1013.

The researchers identified a glucose derivative that binds to an active pocket of GNBP2 and disarms it. This molecule, D-δ-gluconolactone, caused termites to succumb to subsequent infection with the fungus *Metarhizium anisopliae* as well as opportunistic infections in lab tests.

QUANTUM MECHANICS

Do the wave–particle

Nature Phys. doi:10.1038/nphys1278 (2009)

In the whacky world of quantum mechanics, particles can act as waves and waves as particles. Physicists wondered whether this duality might also be true for a form of collective motion known as a 'surface plasmon polariton', which arises when light excites electrons on a metallic surface.

Among other quantum properties, plasmon polaritons seem to have wave–particle behaviour. Fedor Jelezko and Jörg Wrachtrup at the University of Stuttgart in Germany and their colleagues looked at plasma polaritons on the surface of a silver nanowire and found that they interfered with themselves — a telltale signature of wave–particle duality. The authors say the work will prove useful, particularly in the development of quantum networks.

CHEMISTRY

Don't be square

Angew. Chem. Int. Edn **48,** 4824–4827 (2009)

Tiny silver crystals, which among other things are useful as catalysts and in biomedical imaging, like to form as cubes. But to allow better control of their properties, these crystals need to be coaxed into different shapes.

Younan Xia at Washington University in St Louis and his colleagues made silver nanocubes with a conventional reaction using silver nitrate solution, but then quickly added a small, additional amount of this solution. Three of the cubes' faces were augmented with extra silver atoms, creating a crystal that is half octahedron and half truncated cube (pictured below). With slower addition of silver nitrate, the growing cubes remained cubic.

The authors suggest that the exotic crystal shapes could prove useful for an imaging technique called surface-enhanced Raman spectroscopy. Sharp tips, such as the points of an octahedron, help to focus the electric field.

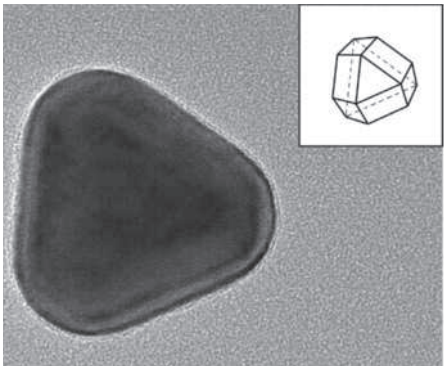

WILEY-VCH

PLANT BIOLOGY

Seeding expression

Science **324,** 1447–1451; 1451–1454 (2009)

The distribution of methyl groups attached to DNA is thought to be the main route by which genes are 'imprinted', or expressed differently depending on the parent from which they are inherited. Two teams reveal that, in the plant *Arabidopsis thaliana*, extensive DNA demethylation occurs in the seed endosperm — the tissue that provides nutrients for the developing embryo — and show how it underlies imprinting.

Steven Henikoff and his colleagues at the Fred Hutchinson Cancer Research Center in Seattle, Washington, used gene-expression and endosperm-demethylation patterns to predict five new imprinted genes. And Robert Fischer, Daniel Zilberman and their colleagues at the University of California, Berkeley, found that extensive hypermethylation in the embryo accompanies endosperm gene demethylation.

The authors suggest that demethylation in the endosperm and production of small RNA molecules helps to silence disruptive transposable elements — short DNA sequences that can copy and insert themselves throughout the genome — in the embryo.

GENE REGULATION

Just-in-time activation

Genes Dev. doi:10.1101/gad.1787109 (2009)

DNA winds around bundles of proteins called histones to make nucleosomes. The histone H2A.Z — a variant of H2A — was thought to prepare genes for activation and then exit the scene once this had occurred. But Luc Gaudreau of the University of Sherbrooke in Canada and his co-workers now show that it is recruited only to the promoter regions of certain genes — those regulated by oestrogen receptor alpha — at around the time of induction. Moreover, recruitment recurs in a cyclical manner, boosting gene expression.

By identifying proteins that bind to specific DNA sequences, the researchers studied the timing of H2A.Z recruitment to a gene promoter after cells were exposed to oestradiol. Compared with H2A, H2A.Z triggers a shift in nucleosome position and stabilizes the binding of other proteins that promote gene expression.

JOURNAL CLUB

Wolf-Dietrich Hardt
ETH Zürich, Switzerland

An infection biologist points out an outstanding issue in mucosal immunology.

The gut immune system can distinguish between harmless commensal microorganisms and dangerous pathogens, and attenuates its response to the former to avoid dangerous chronic inflammation. The mechanisms that maintain this hyporesponsiveness are just beginning to be unravelled.

Dendritic cells, the key organizers of appropriate immune responses, actively sample commensal microbes. In organs other than the gut, this would trigger a strong immune response, and the responsiveness of intestinal dendritic cells to microbes is thought to be thwarted by anti-inflammatory molecules released by gut cells. But the situation could be much more complex: hyporesponsiveness might be restricted to certain 'microbe-associated molecular patterns' (MAMPs), such as lipopolysaccharides, large molecules attached to the outer membrane of many bacteria.

Linda Klavinskis of Kings College London and her team have analysed the MAMP-responsiveness of dendritic cells migrating from gut tissue to local lymph nodes. Surprisingly, these cells do respond to harmless *Bacillus* spores and most MAMPs — but not lipopolysaccharides (V. Cerovic *et al. J. Immunol.* **182,** 2405–2415; 2009). Does this suggest that hyporesponsiveness of intestinal dendritic cells is transient? The maintenance of hyporesponsiveness in the gut mucosa, patterns of MAMP-hyporesponsiveness, and localization and timing of MAMP responses will be important topics for future research.

Unfortunately, unactivated dendritic cells are hard to isolate from the gut mucosa. *In situ* analysis of dendritic-cell responses to gut microbes in intact tissue holds much promise. Technical advances in multicolour two-photon microscopy, fluorescently tagged microbes, and transgenic mice expressing cell-type and response-specific fluorescent reporter proteins will be instrumental in this key area of biology.

Discuss this paper at **http://blogs.nature.com/nature/journalclub**